Mueller & Müller Algorithm Based Synchronisation for Wavelet Packet Modulation

Antony Jamin
Institute for Wireless Networks
RWTH Aachen
Kackertstrasse 9, D-52072 Aachen
Germany
antony.jamin@mobnets.rwth-aachen.de

Petri Mähönen
Institute for Wireless Networks
RWTH Aachen
Kackertstrasse 9, D-52072 Aachen
Germany
petri.mahonen@mobnets.rwth-aachen.de

ABSTRACT

Wavelet packet modulation has been proposed as an interesting alternative to DFT-based multicarrier modulation schemes. Some issues still remain to be addressed for this modulation to be used in practice. This article focuses on the design of a symbol timing tracking algorithm derived from Mueller and Müller work.

Categories and Subject Descriptors

G.1.0 [**General**]: Computer arithmetics—*Numerical algorithms*

General Terms

Design,Algorithms

Keywords

Synchronisation algorithm, multicarrier symbol alignment, wavelet packet modulation

1. INTRODUCTION

Wavelet theory has been foreseen by several authors as a good base on which to build a set of waveform for multicarrier communication [1–3]. In their review on the use of orthogonal transmultiplexers in communications [4], Akansu *et al.* emphasise the relation between filter banks and transmultiplexer theory and predict that wavelet packet modulation (WPM) has a role to play in future communication systems.

The implementation of a working WPM-based transceiver requires the design of a synchronisation method. In this article, we will assume a coarse symbol synchronisation has been achieved using some common techniques. For instance, this can be acheived by inserting a known preamble. We will therefore focus on designing a symbol synchronisation algorithm for WPM. The basic properties of this modulation scheme are first recalled, and the requirements of the sampling synchronisation algorithm are introduced. The details of the proposed sampling phase offset estimation algorithm are given in the third chapter. We then move on to designing the architecture of the closed loop based on this estimator. Some structural modifications are then proposed to improve the tracking performance in the presence of sampling frequency offset. Simulation results are presented in Section 6 to illustrate the performance of our scheme and the effect of the system parameters. Finally, the behaviour of the estimator in case of a multipath channel is emphasised.

IWCMC'06, July 3–6, 2006, Vancouver, British Columbia, Canada.

2. WPM BACKGROUND

Before going into the details of the synchronisation algorithm proposed, we briefly recall the basics of WPM. A WPM-modulated signal generated by a M-point wavelet packet transform can be expressed as [5]

$$s(t) = \sum_{l} \sum_{k=0}^{M-1} a_{l,k} \cdot \varphi_k\Big(t - l\,M\,T_{tr}\Big), \tag{1}$$

where l is the multicarrier symbol index, k is the subcarrier index, φ_k is the k-subcarrier waveform and $a_{l,k}$ is the modulation symbol carried on the k-th subcarrier of the l-th symbol. T_{tr} is the transmitter sampling period. According to Equation 1, consecutive symbols are shifted in time by M sampling period. However, the waveforms φ_k are longer that M samples, hence the consecutive symbols overlap in time.

At the receiver, we obtain the signal $r(t)$

$$r(t) = h(t) * s(t) + n(t), \tag{2}$$

where $h(t)$ denotes the channel impulse response, $n(t)$ is a term representing additive noise and $*$ is the symbol for the convolution operation. The receiver attempts to get an estimate $\widetilde{a}_{l,k}$ of the $a_{l,k}$ from the received signal $r(t)$, i.e.

$$\widetilde{a}_{l,k} = \int_{\tau} r(\tau)\,\widehat{\varphi}_k\big(\tau - \tau_0 - \Delta\tau\big) \quad \delta\tau, \tag{3}$$

where $\Delta\tau$ is the sampling instant offset and τ_0 is a transmitter to receiver delay leading to a perfect synchronisation for $\Delta\tau = 0$. Assuming for the sake of simplicity that the channel response is ideal (i.e. $h(t) = 1$) and the noise $n(t)$

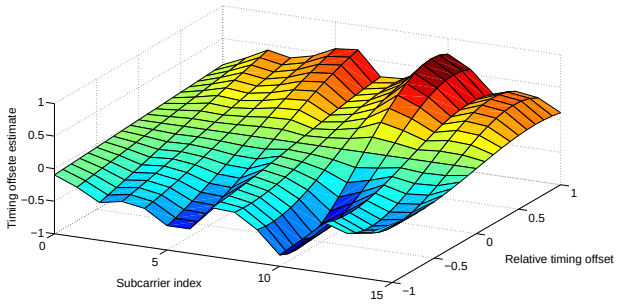

Figure 1: Estimate of timing offset estimate versus actual timing offset for all subcarriers of a 16-point WPM transform WPM signal using Daubechies order 6 wavelet.

is additive white Gaussian, we can rewrite (3) simply as

$$\begin{aligned}\widetilde{a}_{l,k} &= a_{l,k}\cdot\Psi_k(\Delta\tau) \\ &\quad + \sum_{k'=0,\,k'\neq k}^{M-1} a_{l,k'}\cdot\Phi_{k',k}^{l,l}(\Delta\tau) \\ &\quad + \sum_{l'\neq l}\sum_{k'=0}^{M-1} a_{l',k'}\cdot\Phi_{k',k}^{l',l}(\Delta\tau) + n'_{k,l}, \qquad (4)\end{aligned}$$

where $\Psi_k^l(\Delta\tau)$ and $\Phi_{k_1,k_2}^{l_1,l_2}(\Delta\tau)$ are the auto- and cross-waveform detector output values at the erroneous sampling offset $\Delta\tau$, i.e.

$$\Psi_k(\tau) = \int_{-\infty}^{+\infty}\varphi_k^l(t)\,\widehat{\varphi}_k^l(t-\tau)\,dt \qquad (5)$$

$$\Phi_{k_1,k_2}^{l_1,l_2}(\tau) = \int_{-\infty}^{+\infty}\varphi_{k_1}^{l_1}(t)\,\widehat{\varphi}_{k_2}^{l_2}(t-\tau)\,dt. \qquad (6)$$

The first three terms of Equation (4) correspond to three distinct types of interference. There is first a biasing factor in the estimate of the symbol of interest $a_{l,k}$. In a complete system, this bias in the estimate is likely to be compensated by the automatic gain control. The second and third terms are inter-carrier interference and inter-symbol inter-carrier interference contributions respectively. Since WPM is an overlapping modulation scheme, this last term involves a number of multicarrier symbols. This differs from non-overlapping schemes such as OFDM since for them the erroneous sampling instant causes inter-symbols interference only with one adjacent symbol. Finally, $n'_{k,l}$ is the additive noise filtered by the subcarrier waveform φ_k^l.

3. SAMPLING PHASE OFFSET ESTIMATION

The symbol timing offset estimator is a critical element of timing tracking loop. Since the possible applications foreseen for the WPM are portable, highly flexible, wireless devices, we must be able to synchronise at low signal-to-noise ratio (SNR). In addition, it would be interesting if it was capable of tolerating relatively large clock drifts, as that would allow the use of very low cost crystal oscillators.

The requirement of a low working SNR restricts the choice of the estimation algorithm since many exhibit a threshold in the range of 5 to 10 dB, under which the estimator variance is too high to lead to a reliable synchronisation. The Mueller and Müller algorithm [6], originally introduced for single carrier modulation, does not present such a minimal SNR threshold and it has a very low implementation complexity. As many algorithms in estimation theory, it is derived from the maximum likelihood function. The simplest approximation of the algorithm makes use of only two consecutive estimates $\tilde{b}[l-1]$, $\tilde{b}[l]$ and their corresponding symbols after the decision $\hat{b}[l-1]$, $\hat{b}[l]$, i.e.

$$\tilde{\theta}_{MM}[l] = \tilde{b}[l-1]\,\hat{b}[l] - \tilde{b}[l]\,\hat{b}[l-1]\,, \qquad (7)$$

where $\tilde{\theta}_{MM}$ is the estimate of the sampling phase error. Equation (7), using the decision symbols $\hat{b}$, belongs to the family of decision directed algorithms [7, Section 6-2-4]. Of course, known data sequences can be used instead of the decision symbols. This is of particular interest since not having decision errors leads to better performance especially at low SNR. From a practical point of view, this is rather easy to setup with multicarrier schemes as it is common to have some pilot subcarriers modulated with known data symbols.

Since the Mueller and Müller algorithm has been designed for single carrier modulation, its adaptation to the WPM scheme requires further attention. Louveau *et al.* have actually adapted it to the cosine modulated filter bank (CMFB) modulation [8], an alternative overlapping multicarrier modulation. It is however noticeable that their derivation, despite the fact that it is based on empirical analysis, is also valid for other multicarrier schemes, including WPM. Independently of the scheme actually considered, a number of differences with the single carrier case must be emphasised. In multicarrier systems, the modulated symbols are only available at the transform output. Therefore the subcarrier symbols are only available at every M sampling periods T. This leads to a loop delay that is much higher than with typical single carrier scheme, hence limiting the minimum convergence time of the close loop system that would use it. In addition, the subcarriers being by definition centred on a different sub-band of the overall channel, the sampling frequency offset estimation must therefore be evaluated on several subcarriers to increase robustness against frequency selective fading. We must therefore choose how to combine the different estimates. Derivation in [8] has also shown that the sign of the sampling phase estimate is inverted for the subcarriers with even index[1]. Hence, the estimate on those subcarriers having even index must be inverted before com-

[1]Subcarriers are index from 0 to $M-1$, M being the transform size.

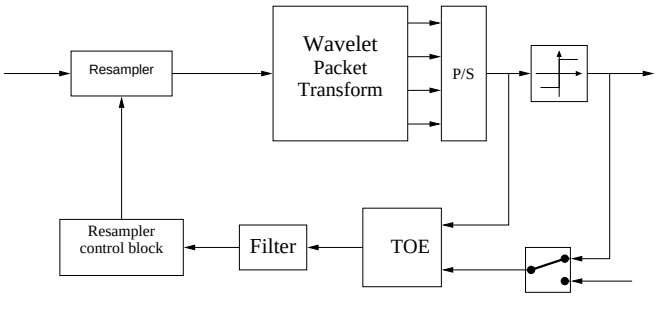

Figure 2: Architecture of the whole digital symbol synchronisation system

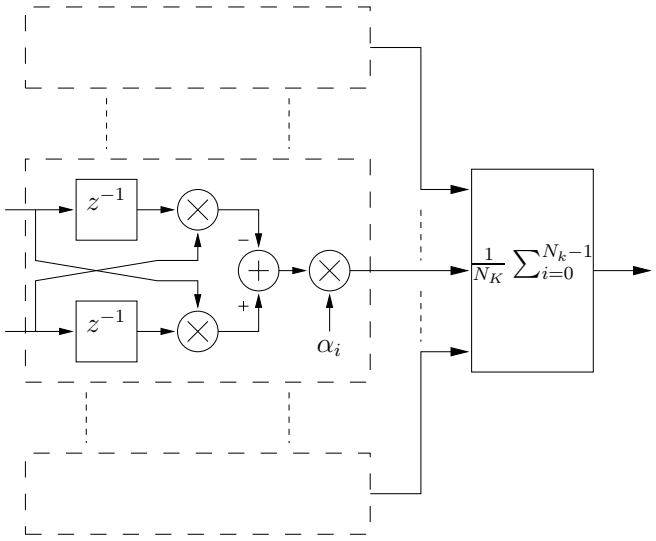

Figure 3: Architecture of the multicarrier timing offset estimator

bination. Taking all these considerations into account, we can express the multicarrier sampling offset estimate $\widetilde{\Delta\tau}$ as

$$\widetilde{\Delta\tau}[l] = \sum_{k\in\mathbb{K}} \alpha_k \cdot (-1)^{k+1} \cdot \widetilde{\delta\tau}_k[l]\,, \tag{8}$$

where $\mathbb{K}$ is the subset of the subcarrier indexes used to estimate the overall timing offset, α_k is a real positive weighing factor of subcarrier k. $\widetilde{\delta\tau}_k[l]$ is the timing error estimate on subcarrier k directly derived from Equation 7 which can be rewritten here as a function of the multicarrier symbols as

$$\widetilde{\delta\tau}_k[l] = \tilde{a}_{l-1,k} \cdot \hat{a}_{l,k} - \tilde{a}_{l,k} \cdot \hat{a}_{l-1,k}\,. \tag{9}$$

The introduction of the weighing factor α_k raises of course the question of how the estimates on the different subcarriers should be combined in order to obtain the final timing offset estimate. To clarify this particular point, Figure 1 plots the estimates $\widetilde{\delta\tau}_k[l]$ of a WPM modulated signal as a function of the actual frequency offset $\delta\tau$ for each subcarrier. This particular case makes use of a 16-point transform of the Daubechies order 4 wavelet. It must be noted that, as discussed in details in [5], the subcarriers have been reordered in such a way that the higher the index k is, the higher the subcarrier centre frequency is. This is important as it clearly emphasises that the slope of the curve and its validity range are related to the position of the centre frequency of the subcarrier. In other words, the subcarriers of lower centre frequency can estimate the timing offset on a wider range, while the subcarriers with a higher centre frequency can estimate the timing offset more accurately. Altogether, this gives us insight in order to decide how to choose the weighting factors α_k. Ultimately, the α_k could be calculated adaptively according to the value of the TOE. At startup time, the range will be favoured. When the system has reached a low TOE and thus would be in tracking mode, the accuracy could be given a higher weight in the overall TOE instead. The approach chosen is intermediate as the γ_k have been chosen in order to have a unity slope for $\delta\tau_0$.

4. CLOSE LOOP DESIGN

The design of a timing offset estimator (TOE) having been largely detailed in the last section, a close loop is now required in order for the receiver to acquire and track this timing offset. The technique proposed in this article is well know as it makes use of a phase locked loop in order to track the best sampling phase. Its overall architecture is depicted in Figure 2. Starting from the wavelet packet transform output, it is composed of the timing offset estimator, a loop filter, a resampler control block and a resampler.

The architecture of the multicarrier timing offset estimator is shown in Figure 3. It has been underlined in the previous section so that the TOE can either be decision driven or data driven. This has been taken into account in Figure 2 by providing the sampling phase offset estimator with both the symbols after decision and some external reference symbols.

Following the TOE is the loop filter. It has two functions in this design. The first is to perform the averaging operation on the noisy TOE output. The second is linked to the operation of a phase locked loop: it controls the loop bandwidth and consequently the dynamic response of the system.

The sampling phase controller is responsible for providing the resampler with the control signals it requires. Namely, the resampler takes as an input a fractional sampling phase μ and symbol shift indicators. Both signals are generated by the sampling phase controller based on the filtered estimate of the timing phase offset. The fractional sampling phase is calculating by integration, i.e.

$$\mu[l+1] = \mathrm{frac}\Big\{\mu[l] - \Gamma_{phase}\,\widetilde{\sigma\tau}[l]\Big\}\,, \tag{10}$$

where $\widetilde{\sigma\tau}[l]$ is $\widetilde{\Delta\tau}[l]$ after going through the loop filter , Γ_{phase} is the phase loop gain and the $frac\{\cdot\}$ returns the fractional part of its argument. The symbol shift indicator $\mu_{shift}[l+1]$ is then in charge to provide the resampler with the additional shift that must be done on its input samples, i.e.

$$\mu_{shift}[l+1] = \begin{cases} -1 & \text{if } \Big(\mu_[l] - \Gamma_{phase}\cdot\widetilde{\sigma_\tau}[l]\Big) \le 0, \\ +1 & \text{if } \Big(\mu_[l] - \Gamma_{phase}\cdot\widetilde{\sigma_\tau}[l]\Big) > 0, \\ 0 & \text{otherwise.} \end{cases} \tag{11}$$

The case where $\mu_{shift}[l]$ is equal to $+1$ (resp. -1) corresponds to the situation where the analog-to-digital converter is providing samples too slowly (resp. too fast) and conse-

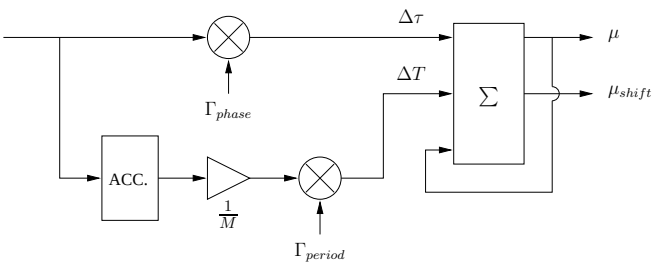

Figure 4: Architecture of the resampler control block

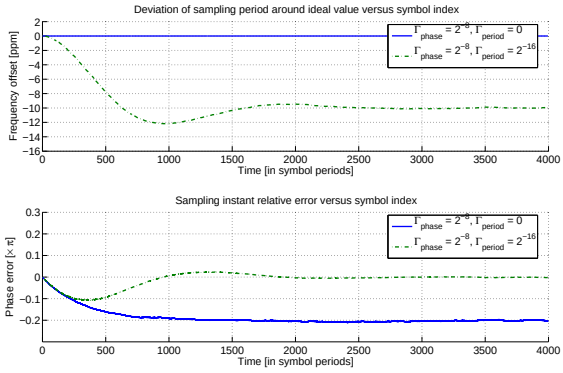

Figure 5: Algorithm performance comparison without and with sampling period estimation. The modulation is 64-point WPM with Daubechies order 6 wavelet. yAll the subcarriers are used for timing estimation, and the loop gains are $\Gamma_{phase} = 2^{-8}$ and $\Gamma_{period} = 2^{-16}$.

quently one input sample should be skipped (resp. used twice).

In order to correct for the sampling phase offset, a digital resampler is used. Its architecture is based on the Farrow structure, with 4 interpolation polynomials of order 3. This corresponds to the case $M = 3, N = 2$ described in details in [9, Section 9.1.3]. Since it is rather difficult to design a resampler with a flat response over the whole frequency band, the signal interpolated is actually sampled at R the modulation Nyquist rate. This looses the requirements on the resampler as its frequency domain response need only to be flat for the normalized frequencies between 0 and in a $\frac{2\pi\omega}{R}$.

5. TRACKING PERFORMANCE IMPROVEMENT

The system described so far is capable of locking accurately on the correct sampling phase when the sampling frequency offset is small enough. In the case of higher sampling period offset, the delay of the tracking loop prevents the loop from reaching a steady state, resulting in the sampling offset estimate to be bias. This is easily understandable since the loop attempts to lock on a sampling phase which is constantly drifting. The actual sampling phase is therefore lagging behind the ideal sampling phase. The remaining sampling phase error is then in proportion to the sampling period offset, the loop total delay and the loop gain. In most applications, this constant sampling phase error is not acceptable as it results in a significant signal distortion, hence limiting the highest SNIR achievable by the system.

A simple way of compensating for the sampling period offset, is to use its estimate $\widetilde{\Delta T}$ in the calculation of the ideal sampling instant $\hat{\mu}[l]$, i.e.

$$\mu[l+1] = \text{frac}\Big\{\mu[l] - \Gamma_{phase}\,\widetilde{\Delta\tau}[l] - \Gamma_{period}\,\widetilde{\Delta T}[l]\Big\}, \quad (12)$$

where Γ_{period} is the sampling period loop gain. Of course, this now leads to the problem of calculating $\widetilde{\Delta T}$. By observing the sampling phase offset is equal to the integral of the period offset, we can write:

$$\widetilde{\Delta T}[l] = \sum_{j=0}^{l-1} \widetilde{\sigma\tau}[j]. \quad (13)$$

Figure 4 shows the simplified architecture of the resulting resampler control block. The addition of the $\frac{1}{M}$ is necessary because the TOE are provided every M clock periods. In practice, this constant is merged together with the loop gain. In system control theory, this modification of the loop is equivalent to adding an *integral* branch to the system, while the phase correction corresponds to the *proportional* branch.

6. SIMULATION RESULTS

This section reports some simulation results in order to illustrate the behaviour of our sampling phase tracking algorithm.

Figure 5 shows for instance the difference in performance when estimating the sampling frequency in addition to the sampling phase. The modulation used is making use of Daubechies order 6 wavelet with 64 subcarriers, all used as reference pilots for the purpose of illustration. The period offset and SNR are set to 10 ppm and 30 dB respectively. For the case with sampling phase estimate only, Γ_{phase} is set equal to 2^{-8} while for the sampling frequency and phase estimate case, Γ_{phase} and Γ_{freq} are set equal to 2^{-8} and 2^{-16} respectively. The estimated sampling period offset versus the multicarrier symbol index is shown in the upper plot. For the case without period estimation, the estimate of the error is of course plotted as constant and null. For the other case, the estimate of the period offset converges towards the ideal value of -10 ppm. The lower plot displays the corresponding sampling phase error. While the first scenario leads to a constant phase offset, the second one is capable of tracking the sampling phase offset, hence leading to a null sampling phase offset.

Figure 6 illustrates the effect of the overall loop delay of the tracking performance of the algorithm. For comparison purpose, a system has been simulated with WPM based on Daubechies wavelets of order 4, 6, 8 and 10 respectively.

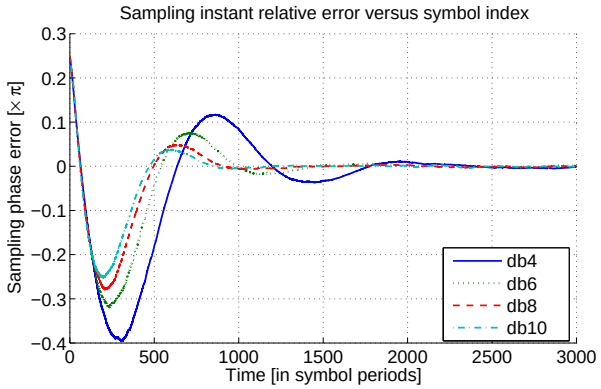

Figure 6: Comparison of sampling phase acquisition time as a function of the wavelet packet length within the Daubechies family. The modulation is 64-point WPM, the SNR is 20 dB, all the subcarriers are used for timing estimation, and the loop gains are $\Gamma_{phase} = 2^{-8}$ and $\Gamma_{period} = 2^{-16}$. The initial normalised phase error was set to 0.25.

With the subcarrier waveforms increasing in order, it can clearly be seen that the system converges to a steady state, with sensibly different damping factors.

As synchronisation procedure usually takes place before equalisation, it is important to analyse the behaviour of any synchronisation scheme in the presence of a channel. For the sake of simplicity, we will assume a simple static frequency channel with a time domain response $h = [0.35\,1\,0.31\,0.07\,-0.04\,0.13\,0.04\,-0.05]$. The upper half of Figure 7 displays the time and frequency responses of this particular channel, while the corresponding S-curve is plotted in its lower half. It can be verified the stable point, corresponding to $\hat{\Delta\tau} = 0$, is slightly offset. By rewriting Equation 4 taking into account the channel response $h(t)$ and ignoring the interference terms, we obtain

$$\widetilde{\Delta\tau}[l]\Big|_{multipath} = h(t) * \widetilde{\Delta\tau}[l]. \qquad (14)$$

An easy way to picture the resulting S-curve is to sum up the time-shifted, weighted version of the ideal channel S-curve. The shift in time and weighing factors corresponds to the delay and amplitude of each tap of the channel impulse response. It must be noticed that in an actual system, this offset does not normally cause significant performance degradation as it should be compensated by the equaliser.

We have shown that the algorithm could work in both data-aided or direction directed mode. The former alternative is obviously most interesting as no bandwidth is lost in transmission of known symbols. On the other hand, in decision directed mode, any decision errors degrade performance of the estimator. This results in increased variance of the estimates at low SNR since this is the region where the errors have the highest probability of occurrence. This is illustrated by Figure 8, where the variance of the estimates for both modes are plotted as a function of the SNR. This particular simulation uses binary amplitude modulation (2-PAM) and here again the modulation is Daubechie order 6 based WPM with weighing factors set for unity slope at origin.

7. CONCLUSION AND FURTHER WORK

We have reported the design and performance of a sampling phase and frequency offset recovery algorithm for WPM signals. The technique used has been adapted from some work carried out for CMFB-based architecture, another overlapping modulation scheme. The overall architecture of the symbol timing tracking algorithm has been described, and its performance in various conditions has been reported. The system has been designed to be capable of working at low SNR and in presence of relatively large clock frequency offset, making it suitable for a wide range of applications.

Further research work remains to be carried out on exploiting the dyadic tree structure which is specific to WPT for synchronisation. In fact, it is likely that making use of the multi-resolution signals internal to the receiver WPT will lead to a synchronisation method with improved characteristics.

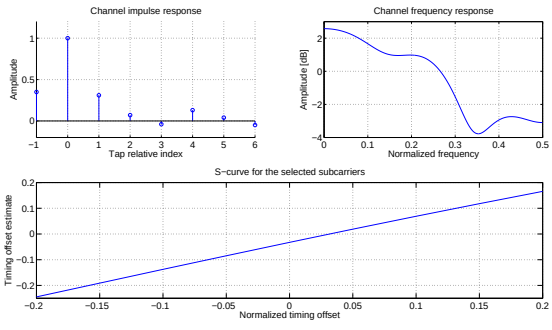

Figure 7: Overall timing offset estimate versus actual timing offset (S-curve) in presence of a multipath static channel. The channel impulse and frequency responses are plotted in the upper part. The system uses a 16-point transform WPM based on Daubechies order 6 wavelet.

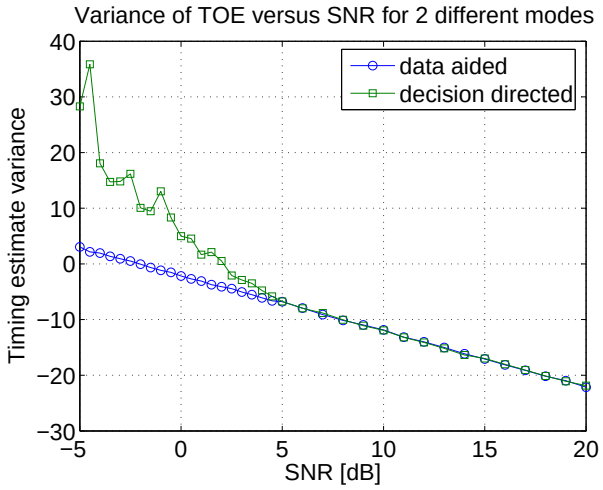

Figure 8: Variance of timing offset estimate versus SNR for data-aided and decision directed modes.The system uses a 16-point transform WPM based on Daubechies order 6 wavelet.

8. REFERENCES

[1] B. G. Negash and H. Nikookar, "Wavelet-based multicarrier transmission over multipath wireless channels," *Electronics Letters*, vol. 36, no. 21, pp. 1787–1788, October 2000.

[2] C. J. Mtika and R. Nunna, "A wavelet-based multicarrier modulation scheme," in *Proceedings of the* 40^{th} *Midwest Symposium on Circuits and Systems*, vol. 2, August 1997, pp. 869–872.

[3] G. W. Wornell, "Emerging applications of multirate signal processing and wavelets in digital communications," in *Proceedings of the IEEE*, vol. 84, 1996, pp. 586–603.

[4] A. Akansu, P. Duhamel, X. Lin, and M. de Courville, "Orthogonal transmultiplexers in communications: a review," *IEEE Transactions on Signal Processing*, vol. 46, no. 4, pp. 979–995, April 1998.

[5] A. Jamin and P. Mähönen, "Wavelet packet based modulation for wireless communications," *Wiley Wireless Communications and Networking Journal*, vol. 5, no. 2, pp. 123–137, March 2005.

[6] K. H. Mueller and M. Müller, "Timing recovery in digital synchronous data receivers," *IEEE Transactions on Communications*, vol. COM-24, no. 5, pp. 516–531, May 1976.

[7] J. G. Proakis, *Digital communications*, 3rd ed. Mc Graw Hill international editions, 1995.

[8] J. Louveaux, L. Cuvelier, L. Vandendorpe, and T. Pollet, "Baud rate timing recovery scheme for filter bank-based multicarrier transmission," *IEEE Transactions on Communications*, vol. 51, no. 4, pp. 652–663, April 2003.

[9] H. Meyr, M. Moeneclaey, and S. A. Fechtel, *Digital communication receivers*. Wiley Interscience, 1997.